RJC

RASĀYAN *J. Chem.*
Vol. 16 | No. 1 |140-146| January - March | 2023
ISSN: 0974-1496 | e-ISSN: 0976-0083 | CODEN: RJCABP
http://www.rasayanjournal.com
http://www.rasayanjournal.co.in

PHOTOCATALYTIC DEGRADATION OF RHODAMINE B UNDER UV USING DOUBLE-LAYER ZnO: Fe THIN FILM

Heri Sutanto[1,3,✉], Ilham Alkian[2,3], Ulfatun Hasanah[1], Eko Hidayanto[1], Indras Marhaendrajaya[1] and Priyono[1]

[1]Department of Physics, Faculty of Science and Mathematics, Diponegoro University, Jawa Tengah 50275, Indonesia

[2]Graduate Program of Environmental Science, School of Postgraduate Studies, Diponegoro University, Jawa Tengah 50241, Indonesia

[3]Smart Materials Research Center (SMARC), Diponegoro University, Jawa Tengah 50275, Indonesia

✉Corresponding Author: herisutanto@live.undip.ac.id

ABSTRACT

Waste dyes are a major source of water pollution, which is a critical environmental issue. The purpose of this study is to synthesize double-layer ZnO: Fe 5-20% thin films and investigate the degradation of rhodamine B in these films. The creation of the ZnO phase with the wurtzite hexagonal structure may be seen in the thin film X-ray diffraction pattern. Only marginally lessened energy bandgap (3.11-3.09 eV), optical transmission spectra, and lattice strain was seen after Fe was added to ZnO thin films. With increasing Fe concentration, it was found that the hydrophilicity and photocatalytic characteristics of ZnO thin films considerably decreased, as shown by the contact angle going from 51.4 to 70.71 and the decomposition efficiency going from 61.46% to 50.35%. The double-layer ZnO layer's optical characteristics diminish as the Fe concentration rises.

Keywords: Double-Layer ZnO: Fe, Photodegradation, Rhodamine B, Thin Film

RASĀYAN *J. Chem.*, Vol. 16, No.1, 2023

INTRODUCTION

Textile industry wastewater is a source of serious water pollution because non-biodegradable dyes contain azo compounds and are carcinogenic. The dyes commonly used in the textile industry are Methylene Blue, Rhodamine B, Methylene Orange, and Direct Red.[1] Azo compounds have the general structure R─N═N─R', where R and R' are the same or different organic chains. Azo compounds can be aliphatic or aromatic compounds that are stable and have fiery colors. Rhodamin B is carcinogenic and mutagenic, so an effective alternative is needed to degrade this compound.[2] Methods such as ozonation, electrocoagulation, membranes, and others require operational costs which are quite expensive, making them less effective in dealing with liquid pollutants. Semiconductor-based photocatalyst methods such as TiO_2, ZnO, CdS, WO_3, and others,[3] are the most effective ways to treat liquid pollutants because they are cost-effective and environmentally friendly, as well as stable. ZnO is an effective and popular n-type semiconductor because it has a higher electron mobility of about 60 MeV at room temperature and a band gap of 3.37 eV.[1,4] The challenge of developing ZnO as a photocatalyst material is related to the wide band gap energy and limited light absorption. The way to reduce the band gap energy is to add doping to improve the optical properties and crystal structure. It is believed that doping using transition metals can reduce the ZnO energy gap and increase the trapping state, such as Cu^{2+}, Co^{2+}, and Fe^{3+}.[5] In this study, Fe was chosen for doping because its ionic radius is not much different from that of Zn in ZnO to facilitate the synthesis process.[6]

Previous research by Sutanto *et al.* reported that single-layer ZnO: Fe thin films had been successfully synthesized and were effective for dye degradation.[7] This study aims to deposit double-layer ZnO: Fe thin films using the sol-gel spray coating method and analyze their photocatalytic ability for dye degradation. The deposited thin layer was characterized using a contact angle meter, X-Ray Diffractometer, and a UV-Vis Spectrophotometer.

http://doi.org/10.31788/RJC.2023.1617061

EXPERIMENTAL

Instruments and Materials

The materials used include Zinc nitrate dehydrate ($Zn(NO_3)_2.4H_2O$) 0.1 M (Sigma Aldrich, 97%), Iron (III) Nitrate ($Fe(NO_3)_3.9H_2O$), Methanol (CH_3OH) (Merck, 99,9%), Acetone (Merck, 99.5%), Aquades, Rhodamin B and glass preparations. The tools used in this research are Compressor (Krisbow, AS 186), VMC digital balance (VB 304), UV-C lamp (20 W), Hotplate Stirrer (Yellow MAG HS 7), UV-Vis Spectrophotometer (Shimadzu UV-Vis 1240 SA), sprayer (Krisbow HS, 1200333), Contact Anglemeter, and X-Ray Diffraction.

Synthesis of ZnO: Fe

The preparation of double-layer ZnO: Fe thin films was carried out by dissolving 0.1 M zinc nitrate dehydrate ($Zn(NO_3)_2.4H_2O$) in 13 ml of distilled water and stirring with a magnetic stirrer at 60 ^oC for 60 minutes until the solution is homogeneous. Preparation of ZnO: Fe solution by adding ZnO solution mixed with Fe doping material sourced from ferrite nitrate ($Fe(NO_3)_3.9H_2O$) with various concentrations of 5, 10, 15, and 20% for 60 minutes at 60 ^oC. The deposition process was carried out at 450 ^oC with a solution of ZnO as the first layer to be deposited, followed by a solution of ZnO: Fe.

Degradation and Characterization

The degradation test was carried out by making a solution of 10 ppm Rhodamine B dye by dissolving 10 mg of Rhodamine B powder into 1 litter of distilled water. The degradation process was carried out for 180 minutes, where every 30 minutes, the dye solution was taken. The degraded dye solution was then characterized using a UV-Vis spectrophotometer with photometric mode to determine its optical properties. The contact angle measurement using a contact angle meter aims to determine the hydrophilicity of the double-layer ZnO: Fe thin film and the XRD test to determine the phase of the constituent material.

RESULTS AND DISCUSSION

Crystal Structure of ZnO: Fe Thin Film

The characterization of the crystal structure of the deposited thin film is shown in Fig.-1. The analysis results at a range of 2θ between 10^o to 90^o show that the diffraction pattern formed in the double-layer ZnO: Fe 5, 10, 15, and 20% thin films corresponded to the ZnO peaks with the hexagonal wurtzite phase (JCPDS No. 36-1451).[8] All of the diffraction peaks that appear show agreement with the diffraction peaks of ZnO. It proves that the thin film deposited does not contain another phase (single phase). The crystal structure of the thin layer of deposition formed is a ZnO polycrystal. The addition of Fe doping causes the peak at an angle of 2θ to change. In general, the peak shift of ZnO has the same pattern, which is shifted to the left (a decrease in angle of 2θ) compared to pure ZnO in the reference. More details can be seen in Fig.-1b. The shift occurs because the addition of the Fe doping concentration causes dislocations in the ZnO crystal so that the atoms are not in their proper position. At the miller index (100) peak widening occurs along with the addition of Fe doping. The widening occurs because the ZnO lattice is deformed by Fe doping.[9] The difference in Fe doping affects the number of diffraction patterns that appear. At the miller index (102) some samples with a specific doping concentration were not observed diffraction peaks but reappeared at the miller index (110). The peak with the Miller index (102) shows that the target atoms are not deposited evenly or homogeneously so the intensity of the diffraction pattern decreases or even disappears (Fig.-1c). This phenomenon causes crystals not to form on the surface, which causes diffraction peaks not to appear. The peak intensity corresponding to the (002) plane was found to decrease with increasing film thickness. This implies that the crystallinity of the ZnO film depends on the purity and grain growth of the material.[10] The effect of Fe doping in the double-layer ZnO: Fe thin film was also analyzed based on the lattice parameters. Table-1 displays the structure parameter data. The lattice parameters a and c change with increasing doping. The lattice parameter a has values from 3.2528-3.2627, and the lattice parameter c has values from 5.2069-5.2090. The lattice parameters a and c are slightly larger than the reference ZnO lattice parameters (JCPDS 36-1451). This difference causes the unit cell volume to increase as well. This lattice shift indicates that Fe doping causes the interstitial or insertion of the ZnO parent compound in the Zn1-xFexO compound composition.[9,10] In addition, changes in lattice parameters affect the volume of the material's unit cell. The volume of the unit cell of the material increases as the lattice parameter increases.

Table-2 also shows the c/a ratio of the double-layer ZnO: Fe thin film of 1.60. The c/a ratio of all doping variations showed conformity with the standard value for pure ZnO with hexagonal wurtzite phase, namely 1.60.[11,12]

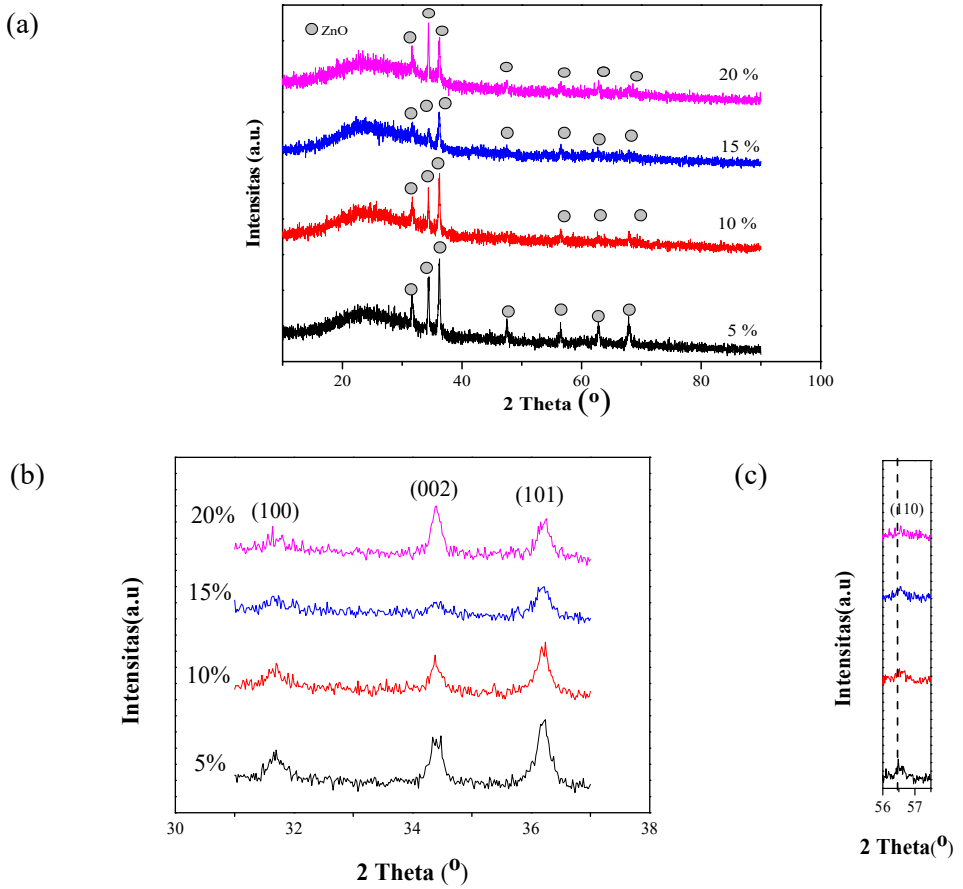

Fig.-1: (a) XRD Test Results (b) 2θ Angle Magnification 31-37° (c) 2θ Angle Magnification 56-58°

Table-1: Lattice Parameters from JCPDS Data (36-1451) and Double-Layer ZnO: Fe Thin Films

ZnO: Fe	*a* (Å)	*c* (Å)	*c/a*	The volume of the unit cell (Å)
5%	3.2600	5.2090	1.60	47.94224
10%	3.2627	5.2090	1.60	48.02234
15%	3.2581	5.2069	1.60	47.86487
20%	3.2528	5.2081	1.60	47.71985
JCPDS 36-1451	3.2490	5.2060	1.60	47.59063

The formation of a double-layer ZnO: Fe thin film with variations in Fe doping was analyzed based on lattice strain. Table-2 shows the lattice strain values using the size strain plot method. The increase in Fe doping reduces the lattice strain value from 8.1569 x 10^{-3} to 4.2621 x 10^{-3}. This phenomenon indicates that Fe is well-doped into ZnO by substitution. However, with the addition of 15% doping concentration in the double-layer ZnO: Fe thin film, there was a very significant increase in the strain value compared to the other thin layers. It indicates that apart from substitution, atomic interstitials also occur due to Fe^{3+} doping. The calculated lattice strain value decreased with increasing Fe concentration, which indicated that a higher concentration of ZnO: Fe film released strain energy by forming larger grains. The value of the film lattice stress has also been found to decrease with increasing Fe concentration, indicating a relaxation of the stresses between the grains and reducing the difference in the coefficient of thermal expansion between the film and the substrate.

Table-2: Strains of Double-Layer ZnO: Fe Based on Size Strain Plot Method

ZnO: Fe (%)	Strain
5	8.1569×10^{-3}
10	8.0507×10^{-3}
15	1.2139×10^{-2}
20	4.2621×10^{-3}

Optical Properties

Optical properties of the double-layer ZnO: Fe thin film analyzed using a UV-Vis spectrophotometer obtained data in an absorbance spectrum. Figure-2 shows that the absorbance of the double-layer ZnO: Fe thin film produces high absorption at a wavelength of 350-375 nm. The maximum absorbance occurs at a wavelength of 358 nm, which is the absorbance of a double-layer thin film with a 5% Fe doping concentration. Based on the absorbance results, it can be seen that the addition of Fe doping in the thin film can shift the absorption wavelength of ZnO so that the absorption area of the material widens and can increase the absorption of the thin layer. The thickness of the double layer also affects absorbance. The thicker the layer (not transparent) formed, the greater the absorbance value.[13] The UV-Vis test results showed that the transparency of the ZnO film decreased with increasing Fe concentration. These results quite support that more photons are absorbed in the ZnO thin film with increasing Fe concentration. Based on Fig.-2, it can be seen that the bandgap energy value decreased along with the addition of Fe doping concentration.

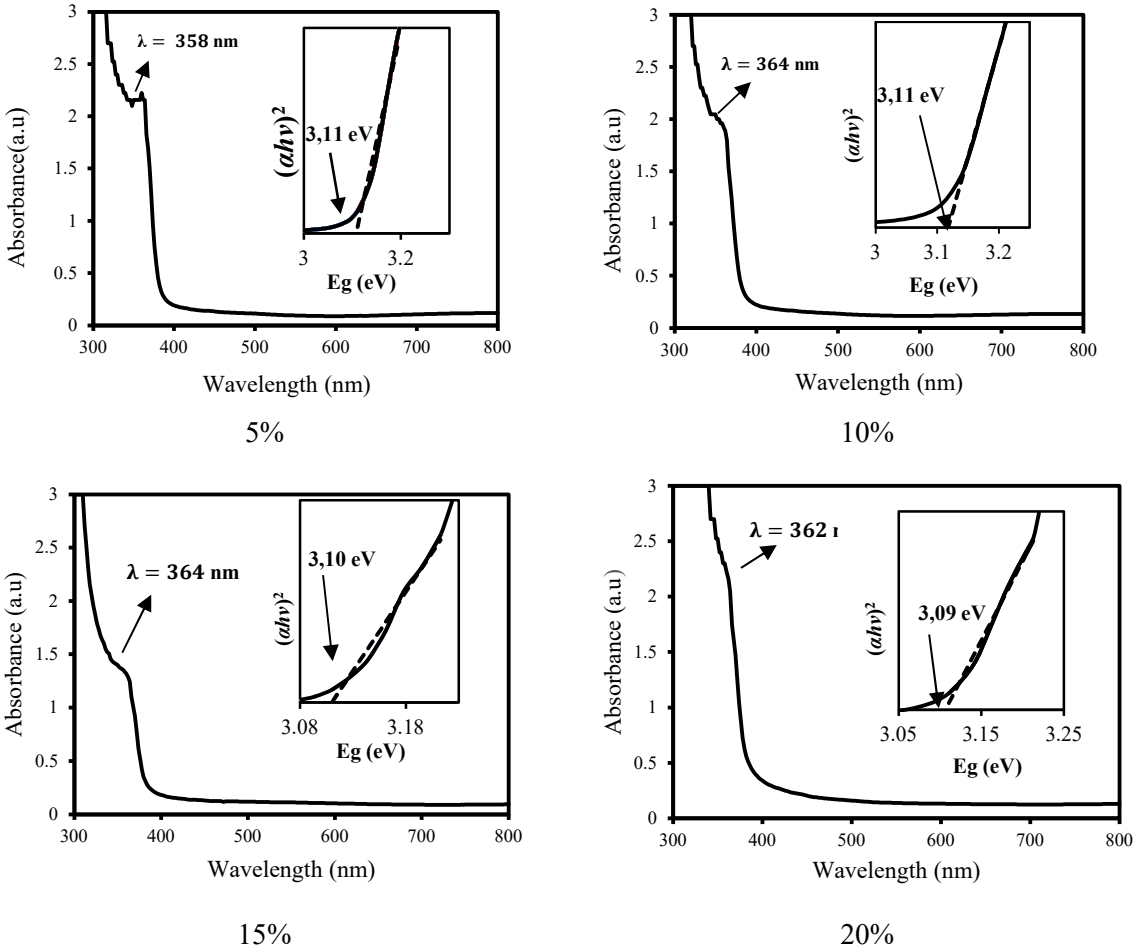

Fig.-2: Absorbance Spectra and Energy Value of the Gap in the Double-Layer ZnO: Fe Thin Film

The smallest band gap energy value is found in a thin layer with a 20% Fe doping concentration of 3.09 eV. The addition of Fe doping on the ZnO thin layer affects a more extended wavelength shift (redshift event). The shift that occurs, namely the redshift, is indicated by a decrease in the bandgap energy as the

concentration of Fe doping increases. This phenomenon occurs because of the excess of electrons, indicating that the Fe into Zn doping process results in a narrowing of the bandgap energy.[11] Bandgap energy decreased slightly (from 3.11 to 3.09 eV) with increasing Fe concentration. The decrease in Eg based on the increase in Fe concentration is consistent with the observed trend in the strain values. The strain value decreases with increasing Fe concentration, which indicates that the strain releases the film at a higher thickness. It was reported that the strain energy changes the distance between the atoms of the semiconductor material and directly affects the energy band gap of the material.[14] The change in the band gap energy of the ZnO thin films may also be related to variations in the mean crystal size of the films.[15,16,17]

Hydrophilicity Analysis

The hydrophilicity of the double-layer ZnO: Fe thin film is said to be hydrophilic (tends to like water) if the angle formed is less than 90°, while it is said to be hydrophobic (does not like water) if the angle formed is more significant than 90°. The test drop solution used was the Rhodamine B solution. Figure-3 is the result of measuring the contact angle of the Rhodamine solution with a double-layer ZnO: Fe thin film. From the data, it can be seen that the value of the contact angle formed increases with the increase in the Fe doping concentration. The slightest contact angle value is formed by a double-layer ZnO: Fe 5% thin film of 51.434°. It is due to the adhesive force that causes the liquid droplets to spread. This adhesive force causes the attractive force between the layer and the solution to get bigger so that the surface angle gets smaller.[18] The contact angle with a small Fe doping concentration indicates that the bonded hydroxyl group is stable to form a hydroxyl multilayer, resulting in a more hydrophilic surface.[19] The hydrophilicity properties increase in proportion to the decrease in the Fe doping concentration caused by the increase in surface energy, thereby increasing the absorption of water molecules on the surface layer. The rate of droplet dispersion between the solution and the layer surface decreases with increasing Fe doping concentration, resulting in agglomeration (buildup), which reduces the hydrophilicity.[20] So the smaller the Fe doping, the higher the hydrophilicity level.[21]

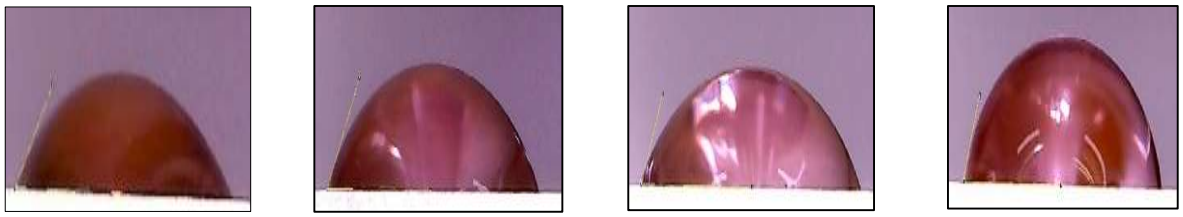

(a) (b) (c) (d)

Fig.-3: Contact Angle of Rhodamine B Solution with ZnO: Fe Thin Film (a) 5%, (b) 10%, (c) 15%, (d) 20%

Photocatalyst Activity

The results are shown in Fig.-5(a) show that the double-layer ZnO: Fe thin film is a photocatalyst material that can reduce organic pollutants. The physical changes in the dye water sample became more apparent, although not too significant, and indicated the success of the photocatalyst process.[22,23] The percentage degradation of the double-layer ZnO: Fe thin film can be observed in Fig.-4(b). Photocatalyst efficiency increases consistently over time. The Rhodamine B degradation graph shows that the 5% Fe doping concentration has the highest degradation rate of 61.45%. The concentration of Fe doping affects the efficiency of the photocatalyst. Double-layer thin films have different transparencies. A double-layer ZnO: Fe 5% thin film had the lowest transparency when viewed based on the absorbance spectrum. The increasingly non-transparent layer causes the thin layer to have a high absorption or absorbance value.[13,14] The degradation results of Rhodamine B with double-layer ZnO: Fe thin film showed a lower degradation ability than our previous study using a ZnO: Fe single layer.[7] This study proves that the thickness of the layer has a significant effect on the degradation process of Rhodamine B. A double layer affects the surface state and the mobility of the surface atoms, thus affecting the efficiency of degradation.[13,24] This result is a very interesting finding because the ZnO: Fe layer with a higher thickness actually results in lower pollutant degradation efficiency. A number of synthesis factors have been regulated the same as in previous studies, including raw material, coating technique, preparation method, substrate area, annealing temperature, and

type of pollutant. ZnO: Fe coating on a substrate that is too thick will inhibit superoxide production and accelerate recombination. On the other hand, in a very thin layer of ZnO: Fe, the production of superoxide is thought to be easier so it interacts more with pollutants. Therefore, the authors recommend developing a method that can grow ZnO: Fe on a substrate with the lowest possible thickness.

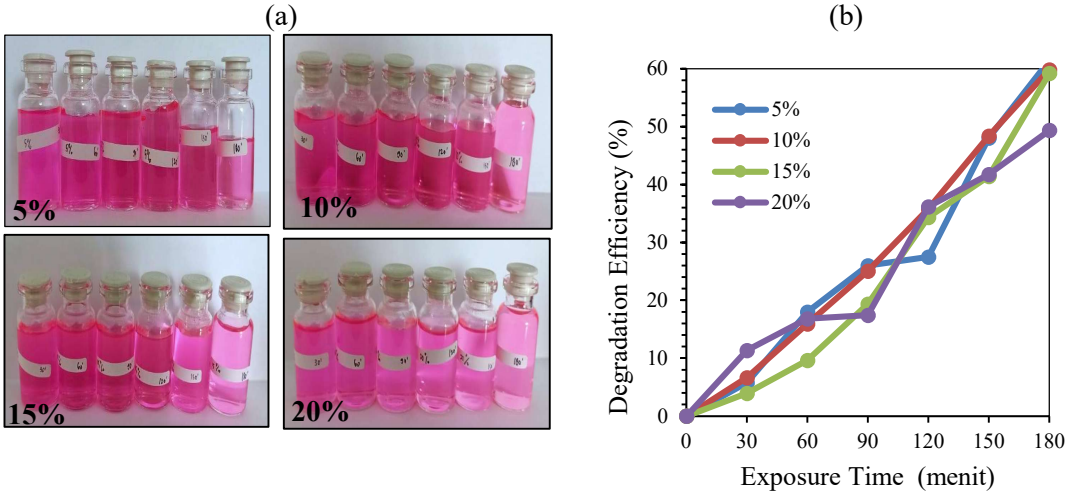

Fig.-5: (a) Change in the Colour of Rhodamine B Degradation Products (b) Rhodamine B degradation Efficiency

CONCLUSION

A double-layer ZnO: Fe thin films were successfully synthesized using the sol-gel spray coating method. The crystal structure formed is hexagonal wurtzite. The variation of Fe doping causes a more minor 2θ angle shift to the left and a larger lattice parameter which indicates that the Fe doping has been successfully inserted into the ZnO parent compound. The addition of Fe doping concentration causes a decrease in bandgap energy, affecting photocatalyst activity. The double-layer ZnO: Fe 5% thin film showed the best hydrophilicity properties. Good hydrophilicity causes high photocatalyst activity in degrading Rhodamine B with a photocatalyst efficiency of 61.46%.

ACKNOWLEDGMENTS

We want to thank the Ministry of Research, Technology, and Higher Education Indonesian for supporting research funding (PDUPT No. 257-59/UN7.6.1/PP/2021)

CONFLICT OF INTERESTS

The authors declare that there is no conflict of interest.

AUTHOR CONTRIBUTIONS

All the authors contributed significantly to this manuscript, participated in reviewing/editing, and approved the final draft for publication. The research profile of the authors can be verified from their ORCID ids, given below:

Heri Sutanto https://orcid.org/0000-0001-7119-9633
Ilham Alkian https://orcid.org/0000-0002-2386-0252
Ulfatun Hasanah https://orcid.org/0000-0001-6719-3415
Eko Hidayanto https://orcid.org/0000-0002-3438-0369
Indras Marhaendrajaya https://orcid.org/0000-0001-8964-3464
Priyono https://orcid.org/0000-0002-0699-0864

REFERENCES

1. E. A. Kumar, W. Tzyy-Jian, and C. Yu-Hsu, *Applied Surface Science,* **585**, 152696(2022), https://doi.org/10.1016/j.apsusc.2022.152696
2. A. Bilgic, *Journal of Alloys and Compounds,* **899**, 163360(2022), https://doi.org/10.1016/j.jallcom.2021.163360
3. Q. Wang, W. Zhang, X. Hu, L. Xu, G. Chen, and X. Li, *Journal of Water Process Engineering*, **40**, 101943(2021), https://doi.org/10.1016/j.jwpe.2021.101943
4. H. Hajighasemi and H. Eshghi, *Materials Science in Semiconductor Processing*, **144**, 106611(2022), https://doi.org/10.1016/j.mssp.2022.106611
5. R. Ge, W. Li, J. Huo, T. Liao, N. Cheng, Y. Du, and J. Zhang, *Applied Catalysis B: Environmental*, **246**, 129(2019), https://doi.org/10.1016/j.apcatb.2019.01.047
6. T. Srinivasulu, Saritha, and R.K.T. Ramakrishna, *Modern Electronic Materials*, **3(2)**, 76(2017), https://doi.org/10.1016/j.moem.2017.07.001
7. H. Sutanto, I. Alkian, V. J. Pramunditya, Mukholit, E. Hidayanto, I. R. Duri, and Priyono, *International Journal of Scientific & Technology Research,* **9(8)**, 315(2020)
8. Z.M. Khoshhesab, M. Sarfaraz, and M.A. Asadabad, *Synthesis and Reactivity in Inorganic Metal-Organic and Nano-Metal Chemistry,* **41**, 814(2011), https://doi.org/10.1080/15533174.2011.591308
9. W. Cheng, and X. Ma, *Journal of Physics: Conference Series,* **152**, 012039(2009), https://doi.org/10.1088/1742-6596/152/1/012039
10. H. Khan, M. Habib, A. Khan, and D. C. Boffito, *Journal of Environmental Chemical Engineering*, **8(5)**, 104282(2020), https://doi.org/10.1016/j.jece.2020.104282
11. S.M. Salaken, J. Podder, and E. Farzama, *Journal of Semiconductors*, **34(7)**, 073003(2013), https://doi.org/10.1088/1674-4926/34/7/073003
12. J.J. Beltran, C.A. Barrero, and A. Punnoose, *Physical Chemistry Chemical Physics,* **17(23)**, 15284(2015), https://doi.org/10.1039/C5CP01408E
13. H. Sutanto, I. Alkian, M. Mukholit, A. A. Nugraha, E. Hidayanto, I. Marhaendrajaya, and Priyono, *Materials Research Express,* **8(11)**, 116402(2021), https://doi.org/10.1088/2053-1591/ac33fe
14. B. A.Utami, H. Sutanto, I. Alkian, F. Sa'Adah, and E. Hidayanto, *Cogent Engineering,* **9**, 2119534(2022), https://doi.org/10.1080/23311916.2022.2119534
15. M. Bouderbala, S. Hamzaoui, M. Adnane, T. Sahraoui, and M. Zerdali, *Thin Solid Films*, **517**, 1572(2009), https://doi.org/10.1016/j.tsf.^{20}08.09.089
16. H.P. He, F. Zhuge, Z.Z. Ye, L.P. Zhu, F.Z. Wang, B.H. Zhao, and J.Y. Huang, *Journal of Applied Physics*, **99**, 023503(2006), https://doi.org/10.1063/1.2161419
17. A.N. Banerjee, C.K. Ghosh, K.K. Chattopadhyay, H. Minoura, A.K. Sarkar, A. Akiba, A. Kamiya, and T. Endo, *Thin Solid Films, Elsevier,* **496,** 112(2006), https://doi.org/10.1016/j.tsf.2005.08.258
18. Berg, J.C., 1993, *Wettability*, CRC Press, New York.
19. S. A. Balta, P. Sotto, L. Luis, B.V. Benea, J. Bruggen, and Kim, *Journal of Membrane Science,* **389**, 155(2012), https://doi.org/10.1016/j.memsci.2011.10.025
20. R. Sakthivel, A. Geetha, B. Anandh and A. S. Ganesh, *Rasayan Journal of Chemistry*, **13(3)**, 1357(2020), https://doi.org/10.31788/RJC.2020.1335562
21. T. Saidani, M. Zaabat, M. S. Aida, and B. Boudine, *Superlattices and Microstructures*, **88**, 315(2015), https://doi.org/10.1016/j.spmi.2015.09.029
22. V. Kumar, S. K. Singh, H. Sharma, S. Kumar, M. K. Banerjee, and A. Vij, *Physica B: Condensed Matter*, **552**, 221(2019), https://doi.org/10.1016/j.physb.2018.10.004
23. A., R. Boughelout, M. Macaluso, Kechouane, and M. Trari, *Reaction Kinetics, Mechanisms and Catalysis,* **129(2)**, 1115(2020), https://doi.org/10.1007/s11144-020-01741-8
24. M. P. Gonullu, *Micro and Nanostructures*, **164**, 107113(2022), https://doi.org/10.1016/j.spmi.2021.107113

[RJC-7061/2022]